Journal of Materials Chemistry C

Accepted Manuscript

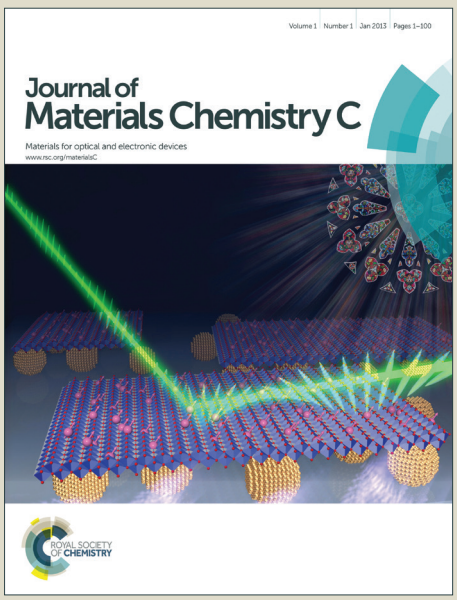

ROYAL SOCIETY OF CHEMISTRY

www.rsc.org/materialsC

Journal Name

COMMUNICATION

Negative induction effect of "graphite" N on graphene quantum dots: tunable band gap photoluminescence

Received 00th January 20xx,
Accepted 00th January 20xx

DOI: 10.1039/x0xx00000x

www.rsc.org/

Chong Zhu [a b c †], Siwei Yang [c †], Gang Wang [c], Runwei Mo [c], Peng He [c], Jing Sun [c], Zengfeng Di [c], Ningyi Yuan [a b], Jianning Ding [a b*], Guqiao Ding [c *], Xiaoming Xie [c]

We demonstrated nitrogen doped graphene quantum dots (N-GQDs) under high temperature of 800-1200 °C and high pressure of 4.0 GPa through a solid-to-solid process. The "graphite" N in N-GQDs has the strong negative induction effect on the band gap. Without the interference of surface groups, the direct band gap of these N-GQDs increased with more nitrogen doping, which results in the tunable photoluminescence (PL) with high PL effeciency. Based on the recognized PL rules, we synthesised the N-GQDs with higher doping concentration and near ultraviolet light-emitting.

Graphene quantum dots (GQDs) have attracted much attention in recent years due to their unique properties and wide range of applications in electrochemical luminescence, photocatalysts, bioimaging, ion detection. [1-4] Previous reported GQDs were synthesised by two broad categories: top-down and bottom-up. [5] The top-down approach involves the cut and/or exfoliation of sp^2 carbon materials, which introduces diverse surface groups on the obtained GQDs. [6-8] Given this fact, the photoluminescence (PL) of tow-down GQDs can be attributed to the n-π* transitions of diversified surface groups. [9, 10] These surface groups play as luminophores, resulting in the excitation wavelength dependence in PL. [9-13] Moreover, these so-called GQDs always show unapparent size effect, which can also be attributed to the surface group PL progress. [9, 12-18] The complicated PL process has made it difficult to clarify band structure, heteroatom contribution to PL and effective control on the PL properties. Recently, there are also several reports about GQDs' bottom-up synthesis using citric acid or other non-aromatic molecules through hydrothermal process, [19] but it is hard to obtain well organized sp^2 carbon arrangement under low temperatures in water. This means that the obtained GQDs also face the same problem as those fabricated through top-down approaches. With precise and multiple-step organic synthesis based on polycyclic aromatic compounds or other molecules with aromatic structures, [14-18] well-defined GQDs with less surface groups can be obtained by bottom-up approach, and these GQDs have given answers to some PL mechanisms. For example, Li *et al.* demonstrated that photoexcited GQDs have a significant probability of relaxing into triplet states, and emit both phosphorescence and fluorescence at room temperature with well-defined GQDs. [18] For GQDs' PL mechanisms, it is still very significant and important to synthesise GQDs without surface groups.

In addition to surface group removing, the bad gap engineering is very critical for modulating of PL emission wavelengths (λ_{em}) and enhancing the PL efficiency (quantum yield, ϕ). [21-28] In theory, a pure band gap PL process will bring very good control on λ_{em} and ϕ. It has been reported that by the negative induction effect of heteroatoms (such as F and N) with high electronegativity, the band gap of GQDs or carbon dots will be broadened effectively. [14, 23] For example, Sun *et al.* reported nitrogen (N) and sulfur (S) co-doped GQDs using citric acid as the C source and urea or thiourea as N and S sources，and the co-doping leads to a high ϕ. [27] Our previous reports also have demonstrated the relationship between the localized π electron cloud and band gap of GQDs. [23, 24] With the high π electron cloud density (by electron injection), the GQDs show narrow band gap and emit redshifted PL. [23, 24] However, GQDs with pure band gap PL without surface group interfaces have not been reported so far.

In this paper, we synthesised nitrogen doped graphene quantum dots (N-GQDs) with tunable band gap, based on the aromatization process of nitrogenous aromatic compound under 800-1200 °C and 4.0 GPa. Due to the high-temperature and high press condition, the GQDs had "graphite" N doping in the lattice without surface groups, which introduces a negative induction effect on the π electron cloud of GQDs and leads to a tunable band gap PL process. These N-GQDs radiated blue, blue-green, yellow and orange PL under UV light with high ϕ (higher than 0.7) when the doping concentration is 5.5, 4.8, 3.5 and 2.4 at. %, respectively. More importantly, we

[a] School of Materials Science and Engineering, Jiangsu Collaborative Innovation Center for Photovolatic Science and Engineering, Jiangsu Province Cultivation base for State Key Laboratory of Photovoltaic Science and Technology, Changzhou University, Changzhou, 213164, Jiangsu, China.
[b] Jiangsu Province Cultivation base for State Key Laboratory of Photovoltaic Science and Technology, Changzhou University, Changzhou, 213164, Jiangsu, China.
[c] State Key Laboratory of Functional Materials for Informatics, Shanghai Institute of Microsystem and Information Technology, Chinese Academy of Science, Shanghai, 200500, China. † Footnotes relating to the title and/or authors should appear here.

Electronic Supplementary Information (ESI) available: [details of any supplementary information available should be included here]. See DOI: 10.1039/x0xx00000x

obtained the near ultraviolet emission N-GQDs with high ϕ (0.86) and good stability through optimizing the doping concentration to 8.2 at. %.

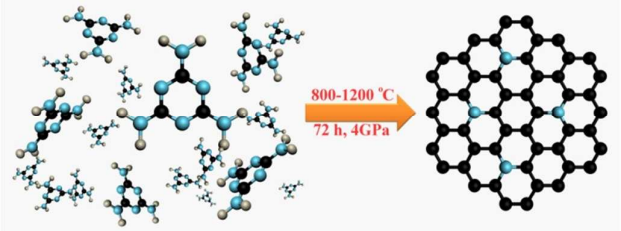

Figure 1 Schematic diagram of the preparation process. The precursor (left) was heated under 800-1200 °C under 4.0 GPa for 72 h. The black and blue spheres represent C and N atoms, respectively.

The preparation process of N-GQDs was run on the piston-cylinder apparatus (Rocktek Instrument) with solid confining media (experimental details are shown in Supporting Information). Typically, melamine powder was put into home-made platinum tube. The pressure was gradually increased to 4.0 GPa, then the sample (Figure S1) were heated for 72 h under 1000 °C (Figure 1). The heating and freezing rates are 100 °C h^{-1}. The press and release rate are 0.2 GPa h^{-1}. After the reaction, the black powder (Figure S2) was obtained and the yield is ~63 wt. %. Although the cost of synthesis is high, the solid to solid process is simple and repeatable. It should be emphasized that all the obtained solids were highly water-soluble with a bath ultrasonication. With the great amount of nucleating points center in solid-phase reaction under high intensity of pressure, the obtained products have uniform size.

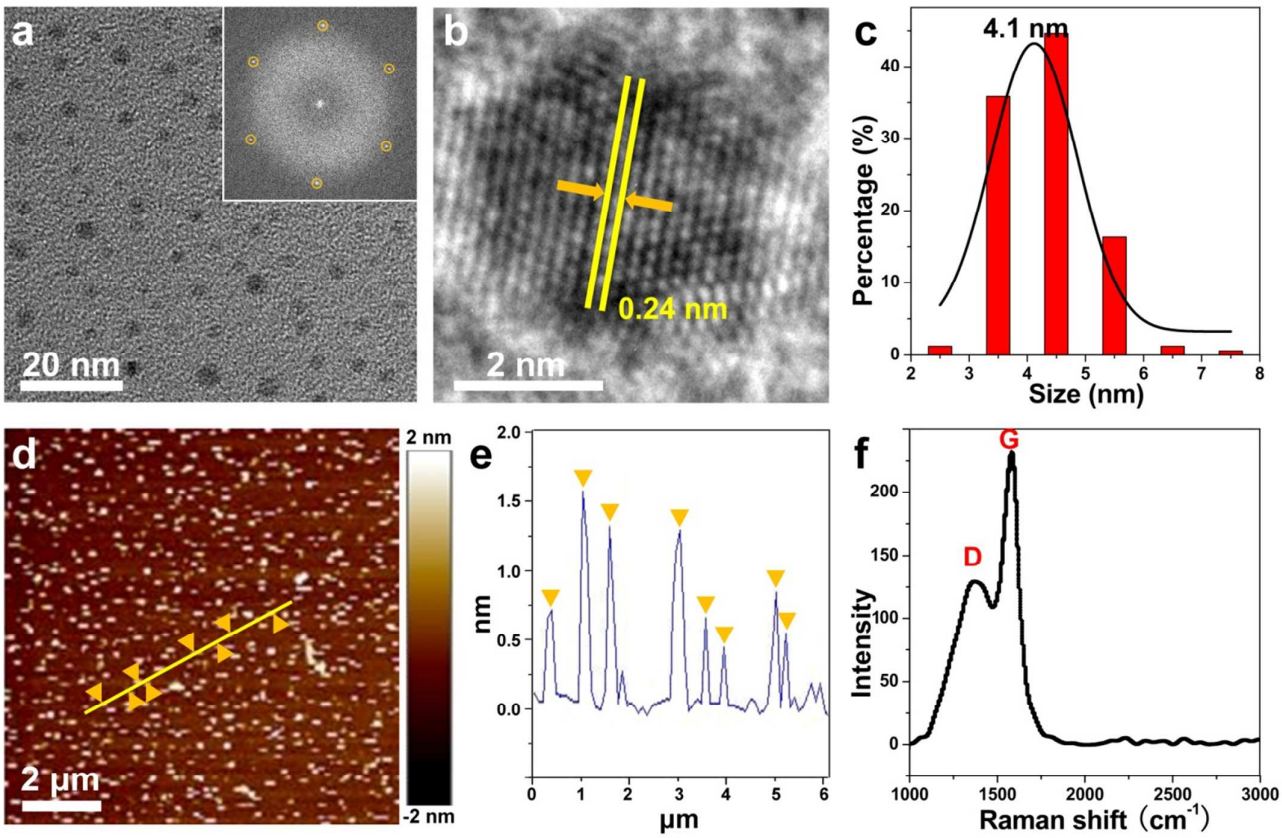

Figure 2 (a) TEM image of N-GQDs thus formed, inset: FFT of a single dot in (a). (b) High-resolution TEM image of a single N-GQD. (c) Corresponding size distribution histogram of N-GQDs, the black curve is the Gaussian fitting curve. (d) AFM topography images of N-GQDs on a mica substrate in tapping mode with the Bruker Dimension Icon AFM microscope, (e) height profile analysis along the line in the image. (f) Raman spectrum of N-GQDs.

Typical characterization results of the as-prepared N-GQDs are shown in Figure 2. Transmission electron microscopy (TEM) images (Figure 2a and b) show fairly uniform N-GQDs with diameter of ca. 2-6 nm. The fast Fourier transform (FFT) (Figure 2a inset) shows a high crystalline structure and significant non-standard six-fold symmetry, indicating the graphene structure of N-GQDs. [22] Clear crystalline lattices fringes are observed from the high-resolution TEM image (Figure 2b). The interlayer spacing of 0.24 nm corresponds to the (1120) lattice fringe of graphene, which matches with previous reports. [32] With the great amount of nucleation points center in solid-phase reaction under high intensity of pressure, the obtained products have uniform size. Corresponding size distribution histogram (Figure 2c) shows the average diameter of these dots is 4.1 nm. Atomic force microscope (AFM) observations (Figure 2 d and e) reveal highly dispersed N-GQDs on the mica substrate with a typical topographic height of 1-1.5 nm, which indicates the 1-2 atomic layer in thickness. [32-34] All the above results indicate the obtained products are GQDs with good crystallinity. Figure 2f presents the Raman spectrum of N-GQDs. The peaks centred at ca. 1368 cm^{-1} and 1384 cm^{-1} attributed to the D

and G band of sp^2 carbon materials, respectively.[35-39] The intensity ratio of the D to G band (I_D/I_G) is approximately 0.41 for the N-GQDs, indicating the good crystalline nature of these as-prepared N-GQDs. [40-42]

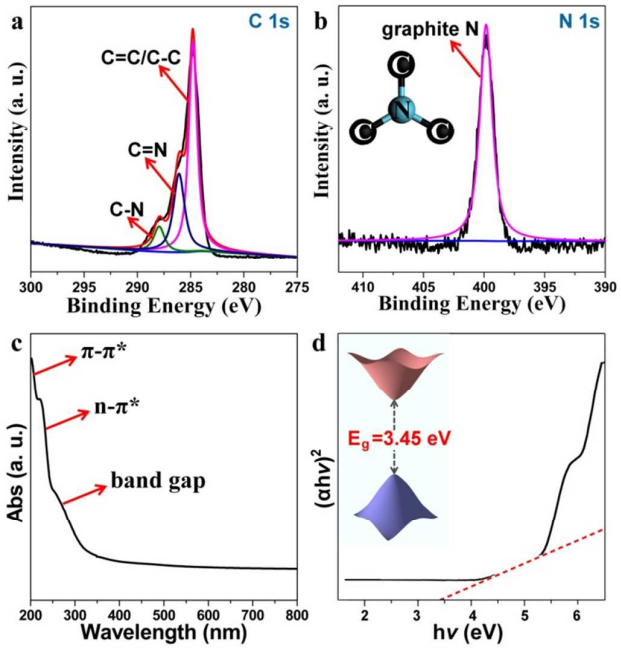

Figure 3 (a) High-resolution C 1s spectrum of the N-GQDs. (b) High-resolution N 1s spectrum of the N-GQDs. (c) UV-vis absorption spectrum of N-GQDs aqueous solution. (d) $(\alpha h\upsilon)^2$ vs. $h\upsilon$ curve of N-GQDs (red trace).

X-ray photoelectron spectroscopy (XPS) measurements were performed to determine the composition of these N-GQDs (Table S1). As shown in Figure S3, a predominant graphite C 1s peak at ca. 284 eV and a N 1s peak at ca. 399 eV are observed. [7, 43, 44, 45] The doping concentration is 4.8 at. %, which is doubly confirmed by elemental analysis (The C/N atomic ratio is 19.2:1, Table S2). The high-resolution C 1s XPS spectrum (Figure 3a) can be divided into three peaks, including C-C/C=C (ca. 284.8 eV), C=N (ca. 286.9 eV) and C-N (ca. 287.8 eV), respectively. [7, 46] The C=N and C-N bonding models can be attributed to the resonant structures of graphitic N. [7, 47] The high-resolution N 1s XPS spectrum (Figure 3b) further characterized the existence form of N. The unimodal N 1s spectrum centred at ca. 400.2 eV corresponding to the "graphitic" N ($(C)_3$-N, including the N atoms in pentagonal, hexagonal or heptagonal structures), which is the unique existence form of N. [7, 48-50, 51] Moreover, the unique $(C)_3$-N bonding model indicates the obtained N-GQDs have no surface groups (such as: $-NH_2$ and -NH). This structure avoids disturbance from other surface groups on PL properties of N-GQDs. Fourier Transform Infrared Spectroscopy (FTIR) was introduced to further characteristic the N-GQDs (Figure S4). Three peaks located in 3170-3440 cm^{-1} can be attributed to the C-H stretching vibrations of benzene ring. [22] Two peaks located in 1496 and 1650 cm^{-1} can be attributed to the C=C and C=N stretching vibrations of pyridines structure (benzene ring with "graphite" N). [22] The peaks located in 415-850 cm^{-1} can be attributed to the ring deformation vibrations of benzene and pyridines rings. [22] The FT-IR results correspond to the XPS results.

The UV-vis absorption spectrum and corresponding optical band gap are shown in Figure 3c and d. The UV-vis absorption spectrum of GQDs (Figure 3c) shows a typical π-π^* transition absorption peak due to aromatic sp^2 domains around 210 nm, [52] an n-π^* transition absorption peak around 240 nm, [53] a band-gap transition absorption peak around 270 nm and a long tail extending into the visible range. [54] The corresponding optical band gap can be estimated from the Tauc plot, i.e. the curve of converted $(\alpha h\nu)^r$ versus $h\nu$ from the UV-visible spectrum, in which α, h, and ν are absorption coefficient, Planck constant, and light frequency, respectively. For an indirect band gap material r=1/2 and a direct band gap material r=2. Figure 3d shows a good linear fit when using r=2, claiming the as-produced N-GQDs are direct band gap materials (no good linear fit is obtained for r=1/2). [54] By measuring the x-axis intercept of an extrapolated line from the linear regime of the curve (Figure 3d, black curve), the band gap energy (E_g) of N-GQDs is 3.45 eV. The large band gap can be due to the strong negative induction effect of "graphite" N in GQDs. [14] Although with 4 electrons in sp^2 orbit, the high electronegativity (3.04) of "graphite" N result the strong negative induction effect, which drastically reduced the π electron cloud of GQDs. The conjugated structure of "graphite" N ensured the above progress. On the other hand, due to the unconjugated structure, the amino and imino groups always show week negative induction effect. [24] Thus, with the low π electron cloud density, the band gap of GQDs is broadened which is just like fluorescent dyes. [24]

To confirm the negative induction effect of "graphite" N on the band gap of these N-GQDs, we synthesised N-GQDs with different doping concentrations by changing the reaction temperature. Due to the decomposition of N-containing groups in higher reaction temperature, [55] the doping concentration decreased with the increased reaction temperature. As shown in Figure 4a, the doping concentration is 5.5, 4.8, 3.5 and 2.4 at. % when the reaction temperature is 900, 1000, 1100 and 1200 ^oC under 4.0 GPa for 48 hours. XPS results show all the N atoms in these N-GQDs are "graphitic" N (Table S1 and 2). Due to the high electronegativity, the corresponding E_g of these N-GQDs is significantly changing with various doping concentrations. The E_g is 3.79, 3.45, 2.91 and 2.38 eV when the doping concentration is 5.5, 4.8, 3.5 and 2.4 at.%, respectively (Figure 4a). All these N-GQDs show good linear fit with $(\alpha h\nu)^2=h\nu$, indicating that these as-prepared N-GQDs are all direct band gap materials (no good linear fit with $(\alpha h\nu)^{1/2}=h\nu$). [54] The proportional relation between the E_g and the content of "graphitic" N demonstrated the strong negative induction effect for the π electron cloud of GQDs.

On the other hand, the tunable direct band gap indicates that these N-GQDs can have controllable wavelength emission with high efficient. Indeed, these N-GQDs radiate bright blue, blue-green, yellow and orange PL under UV light when the doping concentration is 5.5, 4.8, 3.5 and 2.4 at.%, respectively (Figure S5). When the doping concentration is lower, the negative induction effect of "graphite" N is weaker and π electron cloud density is higher, which results in the narrowed band gap. Thus, the corresponding λ_{em} is 402, 436, 495 and 587 nm respectively. The λ_{ex} of these N-GQDs correspond to the band gap transition peak in UV-vis spectra (Table S3), which indicates the PL progress is band gap photoluminescence. All these N-GQDs show strong and sharp

emission peaks (Figure 4b). The full width at half maximum of the PL spectrum is much smaller than it of previously reported GQDs (Figure S6). The weak peak stretch is closely related to not only the homogeneous lateral size, but also the unified band gap PL mechanism. Moreover, due to the transitions of direct band gap, all these N-GQDs show high ϕ over 0.70 (Table S3), which is much higher than that of the most reported GQDs, as the red star marks in Figure 4c among more than 30 literatures marked in dark squares.

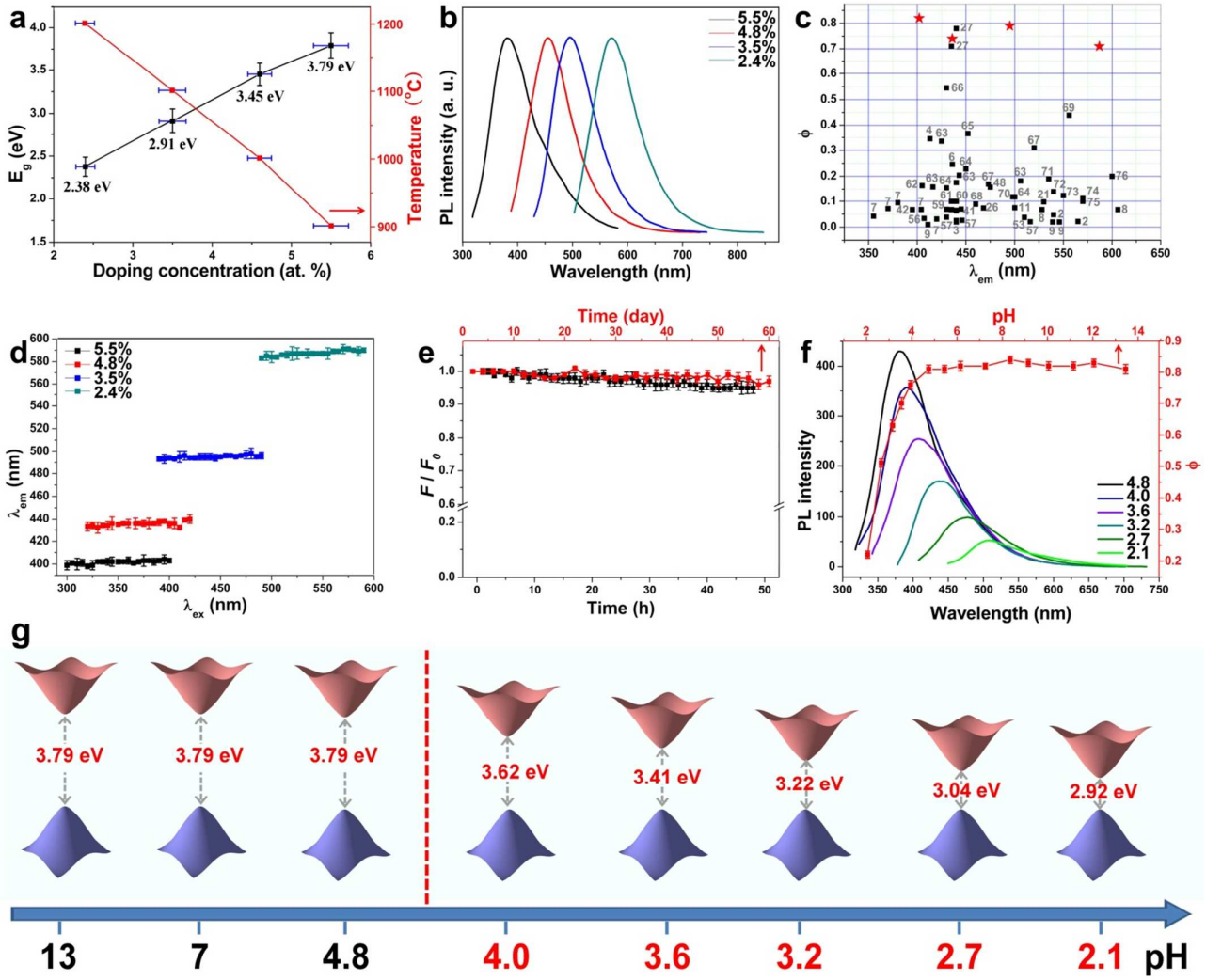

Figure 4 (a) E_g and doping concentrations of N-GQDs under different reaction temperatures. (b) PL spectra of N-GQDs with different doping concentrations. (c) A brief summary of ϕ and λ_{ex} of GQDs. Red stars and black squares represent the results of this work and previous reports, respectively. (d) λ_{em} of N-GQDs with different doping concentrations under different λ_{ex}. (e) The stability N-GQDs under UV light (black curve) and visible light (red curve) at room temperature. The *F* and F_0 are PL intensity of N-GQDs (doping concentration: 5.5 at. %) when t=0 and at corresponding times, respectively. The concentration of N-GQDs aqueous solution is 0.1 mg mL^{-1}. (f) PL spectra and ϕ (red curve) of N-GQDs (doping concentration: 5.5 at.%) under different pH. (g) E_g of N-GQDs (doping concentration: 5.5 at.%) under different pH. The concentration of N-GQDs aqueous solution is 0.1 mg mL^{-1}.

The band gap PL progress also results in different PL performances compared to previously reported GQDs with diversified surface groups. As shown in Figure 4d, these N-GQDs show excitation wavelength independence with the change of λ_{ex}. All these N-GQDs exhibit a maxima λ_{em} shift of 10 nm when the excitation wavelength changed. Due to the stable "graphitic" N, these N-GQDs exhibit excellent photo stability. No obvious change in PL intensity (Figure 4e and Figure S7-9) is observed under UV light (centre wavelength of 325 nm) for 48 h or visible light for more than 60 days. What's more, it is interesting that these N-GQDs exhibit red shifted PL and decreased ϕ with the increasing acidity of the solution (Figure 4f and Figure S10-12). Taking the N-GQDs with 5.5 at.% doping concentration as an example, the λ_{em} and ϕ show no obvious change when in weak acid, neutral and basic medium (pH: 4.5-14). However, when the pH is 4.0, 3.6, 3.2, 2.7 and 2.1, the λ_{em} is 391, 406, 438, 472 and 507 nm, respectively (Figure 4f). The corresponding E_g is 3.62, 3.41, 3.22, 3.04 and 2.92 eV, when the pH is 4.0, 3.6, 3.2, 2.7 and 2.1 respectively (Figure 4g). When these N-GQDs in acid environment the "graphitic" N protonated gradually. These protonated "graphitic" N show weaker negative induction effect than that of un-protonated "graphitic" N under the function of protons. [77, 78] This results in the high π electron cloud density,

which means the narrowed band gap. With the narrowed band gap, the PL spectrum was red shifted. On the other hand, the protonated "graphitic" N also results in the non-planar structure, leading to increased the energy loss and the decreased quantum yield. Moreover, the change of PL properties of N-GQDs indicates that they may be used as fluorescence probes for environment. Furthermore, the ϕ is 0.76, 0.70, 0.63, 0.51 and 0.22 when the pH is 4.0, 3.6, 3.2, 2.7 and 2.1, respectively, which can be due to the increased flexible of protonated molecular structure. The flexible molecular structure results in the increasing non-radiation transitions and molecular vibration. [79-81]

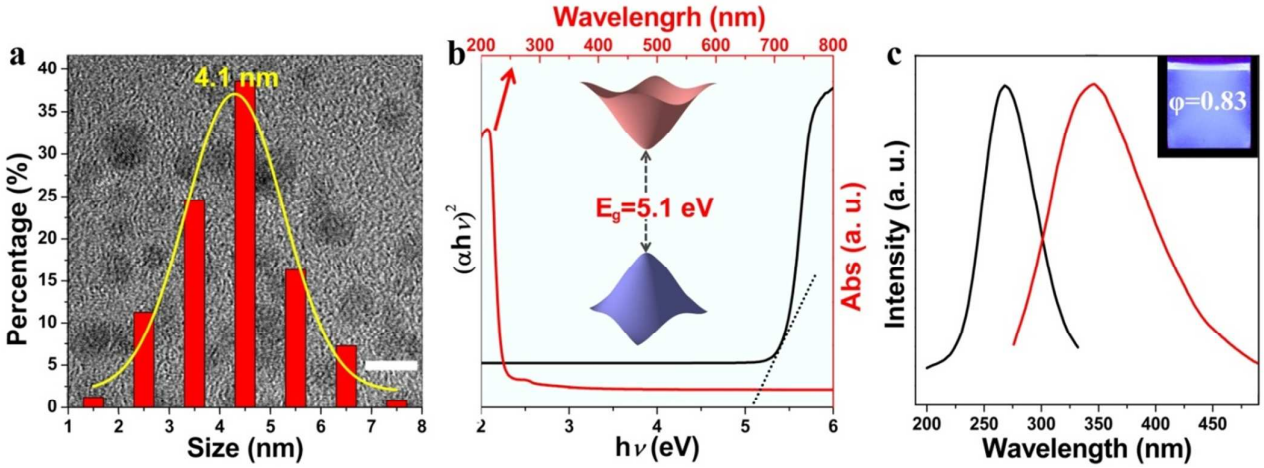

Figure 5 (a) TEM image and corresponding size distribution histogram of near ultraviolet emitted N-GQDs thus formed (scale bar: 5 nm). (b) UV-vis absorption spectrum (black trace) and $(\alpha h\upsilon)^2$ vs. $h\upsilon$ curve (red trace) of N-GQDs aqueous solution. (c) PL and PLE spectra of near ultraviolet emitted N-GQDs aqueous solution. Inset shows the digital photo of N-GQDs aqueous solution under and 365 nm UV light.

Finally, based on above surely recognized rules, we synthesised the N-GQDs with higher doping concentration under lower temperature on the premise of complete reaction (Figure 5a). When the reaction temperature is 800 ^{o}C, the doping concentration of N-GQDs is 6.4 at. % (XPS results were shown in Table S1 and 2). The E_g of N-GQDs is 5.1 eV through calculation (Figure 5b). The photoluminescence excitation (PLE) and PL spectra in Figure 5c show that the optimum excitation and emission wavelength is 268 nm and 344 nm, which is much shorter than that of N-GQDs in the previous reports (Figure S6). [82-88] As an direct band gap material, as well as other N-GQDs with lower doping concentrations, these N-GQDs also show high ϕ of 0.83. Moreover, the as-prepared N-GQDs have excellent stability (Figure S13 and 14). Stronger negative induction effect of more "graphite" N broadens the band gap, and results in high ϕ and near ultraviolet band-gap PL, which indicates that these obtained N-GQDs may be used as near ultraviolet light-emitting materials.

Conclusions

In summary, we synthesised the N-GQDs without surface groups under high temperature over 800 ^{o}C and high pressure. All N atoms in these N-GQDs are "graphite" N, and the doping concentration can be easily controlled through changing the reaction temperature. Without the Interference of surface groups, the direct band gap of these N-GQDs show regularly changes, which results in a tunable PL with high quantum yield. The change of band gap could be due to the strong negative induction effect of "graphite" N. Based on recognized PL rules, we synthesised the N-GQDs with higher doping concentration, which show high-efficient near ultraviolet light-emitting with good stability.

Acknowledgements

This work was supported by projects from the National Science and Technology Major Project (2011ZX02707), the Chinese Academy of Sciences (KGZD-EW-303 and XDA02040000), the Jiangsu Province Cultivation base for State Key Laboratory of Photovoltaic Science and Technology (201508).

Notes and references

† *These authors (Chong Zhu and Siwei Yang) contributed equally.*
* *Corresponding authors: Jianning Ding, dingjn@cczu.edu.cn; Guqiao Ding, gqding@mail.sim.ac.cn.*

1 L. A. Ponomarenko, F. Schedin, M. I. Katsnelson, R. Yang, E. W. Hill, K. S. Novoselov and A. K. Geiml, *Science*, 2008, **320**, 356.
2 L. Zhou, J. L. Geng and B. Liu, *Part. Part. Syst. Charact.*, 2013, **30**, 1086.
3 R. Gokhale and P. Singh, *Part. Part. Syst. Charact.*, 2014, **31**, 433.
4 Y. Q. Dai, H. Long, X. T. Wang, Y. M. Wang, Q. Gu, W. Jiang, Y. C. Wang, C. C. Li, T. T. Helen Zeng, Y. M. Sun and J. Zeng, *Part. Part. Syst. Charact.*, 2014, **31**, 597.
5 M. Bacon, S. J. Bradley and T. Nann, *Part. Part. Syst. Charact.*, 2014, **31**, 415.
6 C. F. Hu, Y. L. Liu, Y. H. Yang, J. H. Cui, Z. R. Huang, Y. L. Wang, L. F. Yang, H. B. Wang, Y. Xiao and J. H. Rong, *J. Mater. Chem. B*, 2013, **1**, 39.
7 F. Yang, M. L. Zhao, B. Z. Zheng, D. Xiao, L. Wu and Y. Guo, *J. Mater. Chem.*, 2012, **22**, 25471.
8 X. M. Li, S. P. Lau, L. B. Tang, R. B. Jic and P. Z. Yang, *J. Mater. Chem. C*, 2013, **1**, 7308.
9 R. Sekiya, Y. Uemura, H. Murakami and T. Haino, *Angew. Chem. Int. Ed.*, 2014, **53**, 5619.

10 D. B. Shinde and V. K. Pillai, *Angew. Chem. Int. Ed.*, 2013, **52**, 2482.
11 D. Y. Pan, L. Guo, J. C. Zhang, C. Xi, Q. Xue, H. Huang, J. H. Li, Z. W. Zhang, W. J. Yu, Z. W. Chen, Z. Li and M. H. Wu, *J. Mater. Chem.*, 2012, **22**, 3314.
12 R. Q. Ye, C. S. Xiang, J. Lin, Z. W. Peng, K. W. Huang, Z. Yan, P. C. Nathan, L. G. Erro Samuel, C. C. Hwang, G. D. Ruan, G. Ceriotti, A. R. O. Raji, A. A. Martí and M. T. James, *Nat. Commun.*, 2013, **4**, 2943.
13 J. C. Ge, M. H. Lan, B. J. Zhou, W. M. Liu, L. Guo, H. Wang, Q. Y. Jia, G. L. Niu, X. Huang, H. Y. Zhou, X. M. Meng, P. F. Wang, C. S. Lee, W. J. Zhang and X. D. Han, *Nat. Commun.*, 2014, **5**, 4596.
14 M. J. Allen, V. C. Tung and R. B. Kaner, *Chem. Rev.*, 2010, **110**, 132.
15 H. L. Qian, F. Negri, C. R. Wang and Z. H. Wang, *J. Am. Chem. Soc.*, 2008, **130**, 17970.
16 D. Niedzialek, V. Lemaur, D. Dudenko, J. Shu, M. R. Hansen, J. W. Andreasen, W. Pisula, K. Müllen, J. Cornil and D. Beljonne, *Adv. Mater.*, 2013, **25**, 1939.
17 Q. Q. Li, S. Zhang, L. M. Dai and L. S. Li, *J. Am. Chem. Soc.*, 2012, **134**, 18932.
18 M. L. Mueller, X. Yan, J. A. McGuire and L. S. Li, *Nano Lett.*, 2010, **10**, 2679.
19 L. Wang, Y. L. Wang, T. Xu, H. B. Liao, C. J. Yao, Y. Liu, Z. Li, Z. W. Chen, D. Y. Pan, L. T. Sun and M. H. Wu, *Nat. Commun.*, 2014, **5**, 5357.
20 M. Bacon, S. J. Bradley and T. Nann, *Part. Part. Syst. Charact.*, 2014, **31**, 415.
21 X. H. Zhu, X. Xiao, X. X. Zuo, Y. Liang and J. M. Nan, *Part. Part. Syst. Charact.*, 2014, **31**, 801.
22 J. Sun, S. W. Yang, Z. Y. Wang, H. Shen, T. Xu, L. T. Sun, H. Li, W. W. Chen, X. Y. Jiang, G. Q. Ding, Z. H. Kang, X. M. Xie and M. H. Jiang, *Part. Part. Syst. Charact.*, 2015, **32**, 434.
23 S. W. Yang, J. Sun, X. B. Li, W. Zhou, Z. Y. Wang, P. He, G. Q. Ding, X. M. Xie, Z. H. Kang and M. H. Jiang, *J. Mater. Chem. A*, 2014, **2**, 8660.
24 S. W. Yang, J. Sun, P. He, X. X. Deng, Z. Y. Wang, C. Y. Hu, G. Q. Ding and X. M. Xie, *Chem. Mater.*, 2015, **27**, 2004.
25 S. W. Yang, C. Zhu, J. Sun, P. He, N. Yuan, J. Ding, G. Ding and X. Xie, *RSC Adv.*, 2015, **5**, 33347.
26 J. H. Shen, Y. H. Zhu, C. Chen, X. L. Yang and C. Z. Li, *Chem. Commun.*, 2011, **47**, 2580.
27 D. Qu, M. Zheng, P. Du, Y. Zhou, L. G. Zhang, D. Li, H. Q. Tan, Z. Zhao, Z. G. Xie and Z. C. Sun, *Nanoscale*, 2013, **5**, 12272.
28 D. Wang, J. F. Chen and L. M. Dai, *Part. Part. Syst. Charact.*, 2015, **32**, 515.
29 J. H. Shen, Y. H. Zhu, X. L. Yang and C. Z. Li, *Chem. Commun.*, 2012, **48**, 3686.
30 C. Gong, J. M. Jiang, C. Li, L. W. Song, Z. N. Zeng, J. Miao, X. C. Ge, Y. H. Zheng, R. X. Li and Z. Z. Xu, *Phys. Rev. A*, 2012, **85**, 33410.
31 C. M. Luk, L. B. Tang, W. F. Zhang, S. F. Yu, K. S. Teng and S. P. Lau, *J. Mater. Chem.*, 2012, **22,** 22378.
32 X. B. Li, S. W. Yang, J. Sun, P. He, X. P. Pu and G. Q. Ding, *Synth. Met.*, 2014, **194**, 52.
33 X. B. Li, S. W. Yang, J. Sun, P. He, X. G. Xu and G. Q. Ding, *Carbon*, 2014, **78**, 38.
34 P. He, C. Zhou, S. Y. Tian, J. Sun, S. W. Yang, G. Q. Ding, X. M. Xie and M. H. Jiang, *Chem. Commun.*, 2015, **51**, 4651.
35 W. L. Xing, G. Lalwani, I. Rusakova and B. Sitharaman, *Part. Part. Syst. Charact.*,2014, **31**, 745.
36 G. Abellan, E. Coronado, C. Marti-Gastaldo, A. Ribera, T. F. Otero, *Part. Part. Syst. Charact.*, 2013, **30**, 853.
37 C. Galande, W. Gao, A. Mathkar, A. M. Dattelbaum, T. N. Narayanan, A. D. Mohite and P. M. Ajayan, *Part. Part. Syst. Charact.*, 2014, **31**, 619.
38 T. L. Moore, R. Podilakrishna, A. Rao and F. Alexis, *Part. Part. Syst. Charact.*, 2014, **31**, 886.
39 J. Dong, Q. Yang and J. Weng, *Part. Part. Syst. Charact.*, 2014, **31**, 1072.
40 P. He, J. Sun, S. Y. Tian, S. W. Yang, S. J. Ding, G. Q. Ding, X. M. Xie and M. H. Jiang, *Chem. Mater.*, 2015, **27**, 218.
41 P. Atienzar, A. Primo, C. Lavorato, R. Molinari and H. Garcia, *Langmuir*, 2013, **29**, 6141.
42 C. X. Li, D. Y. Jiang, L. L. Zhang, J. F. Xia and Q. Li, *Langmuir*, 2012, **28**, 9729.
43 C. Chen, L. J. Wang, Y. Y. Liu, Z. W. Chen, D. Y. Pan, Z. Li, Z. Jiao, P. F. Hu, C. H. Shek, C. M. L. Wu, J. K. L. Lai and M. H. Wu, *Langmuir*, 2013, **29**, 4111.
44 S. W. Yang, S. Huang, D. Liu and F. Liao, *Synth. Met.*, 2012, **162**, 2228.
45 F. Liao, S. Yang, X. Li, L. Yang, Z. Xie, C. Hu, S. Yan, T. Ren and Z. Liu, *Synth. Met.*, 2014, **189**, 126.
46 X. Song, S. Yang, L. He, S. Yan and F. Liao, *RSC Adv.*, 2014, **4**, 49000.
47 F. Liao and S. W. Yang, *Synth. Met.*, 2015, **205**, 32.
48 M. B. Wu, Y. Wang, W. T. Wu, C. Hu, X. N. Wang, J. T. Zheng, Z. T. Li, B. Jiang and J. S. Qiu, *Carbon*, 2014, **78**, 480.
49 F. Liao, X. Song, S. W. Yang, C. Y. Hu, L. He, S. Yan and G. Q. Ding, *J. Mater. Chem. A*, 2015, **3**, 7568.
50 S. Yan, S. W. Yang, L. He, C. C. Ye, X. Song and F. Liao, *Synth. Met.*, 2014, **198**, 142.
51 S. Yang, C. Ye, X. Song, L. He, S. Yan and F. Liao, *RSC Adv.*, 2014, **4**, 54810.
52 X. Yan, Q. Q. Li and L. S. Li, *J. Am. Chem. Soc.*, 2012, **134**, 16095.
53 R. L. Liu, D. Q. Wu, X. L. Feng and K. Müllen, *J. Am. Chem. Soc.*, 2011, **133**, 15221.
54 J. Liu, Y. Liu, N. Y. Liu, Y. Z. Han, X. Zhang, H. Huang, Y. Lifshitz, S. T. Lee, J. Zhong and Z. H. Kang, *Science*, 2015, **347**, 970.
55 H. M. Zhang, Y. Wang, D. Wang, Y. B. Li, X. L. Liu, P. Liu, H. G. Yang, T. C. An, Z. Y. Tang and H. J. Zhao, *Small*, 2014, **10**, 3371.
56 S. J. Zhuo, M. W. Shao and S. T. Lee, *Acs Nano*, 2012, **6**, 1059.
57 S. J. Zhu, J. H. Zhang, S. J. Tang, C. Y. Qiao, L. Wang, H. Y. Wang, X. Liu, B. Li, Y. F. Li, W. L. Yu, X. F. Wang, H. C. Sun and B. Yang, *Adv. Funct. Mater.*, 2012, **22**, 4732.
58 D. B. Shinde and V. K. Pillai, *Chem. Eur. J.*, 2012, **18**, 12522.
59 D. Y. Pan, J. C. Zhang, Z. Li and M. H. Wu, *Adv. Mater.*, 2010, **22**, 734.
60 A. Ananthanarayanan, X. W. Wang, P. Routh, B. Sana, S. Lim, D. H. Kim, K. H. Lim, J. Li and P. Chen, *Adv. Funct. Mater.*, 2014, **24**, 3021.
61 W. Kwon, Y. H. Kim, C. L. Lee, M. Lee, H. C. Choi, T. W. Lee and S. W. Rhee, *Nano Lett.*, 2014, **14**, 1306.
62 H. J. Sun, N. Gao, L. Wu, J. S. Ren, W. L. Wei and X. G. Qu, *Chem. Eur. J.*, 2013, **19**, 13362.
63 Z. S. Qian, X. Y. Shan, L. J. Chai, J. R. Chen and H. Feng, *Nanotechnology*, 2014, **25**, 415501.
64 L. L. Li, J. Ji, R. Fei, C. Z. Wang, Q. Lu, J. R. Zhang, L. P. Jiang and J. J. Zhu, *Adv. Funct. Mater.*, 2012, **22**, 2971.
65 Z. L. Wu, M. X. Gao, T. T. Wang, X. Y. Wan, L. L. Zheng and C. Z. Huang, *Nanoscale*, 2014, **6**, 3868.
66 X. Wu, F. Tian, W. X. Wang, J. Chen, M. Wu and J. X. J. Zhao, *J. Mater. Chem. C*, 2013, **1**, 4676.
67 X. Liu, H. J. Liu, F. Cheng and Y. Chen, *Nanoscale*, 2014, **6**, 7453.
68 Y. Q. Dong, G. L. Li, N. N. Zhou, R. X. Wang, Y. W. Chi and G. N. Chen, *Anal. Chem.*, 2012, **84**, 8378.
69 Y. P. Hu, J. Yang, J. W. Tian, L. Jia, J. S. Yu, *Carbon*, 2014, **77**, 775.
70 J. Peng, W. Gao, B. K. Gupta, Z. Liu, R. Romero-Aburto, L. H. Ge, L. Song, L. B. Alemany, X. B. Zhan, G. H. Gao, S. A.

Vithayathil, B. A. Kaipparettu, A. A. Marti, T. Hayashi, J. J. Zhu and P. M. Ajayan, *Nano Lett.*, 2012, **12**, 844.
71 H. Tetsuka, R. Asahi, A. Nagoya, K. Okamoto, I. Tajima, R. Ohta and A. Okamoto, *Adv. Mater.*, 2012, **24**, 5333.
72 M. Zhang, L. L. Bai, W. H. Shang, W. J. Xie, H. Ma, Y. Y. Fu, D. C. Fang, H. Sun, L. Z. Fan, M. Han, C. M. Liu and S. H. Yang, *J. Mater. Chem.*, 2012, **22**, 7461.
73 S. Chen, X. Hai, C. Xia, X. W. Chen and J. H. Wang, *Chem. Eur. J.*, 2013, **19**, 15918.
74 L. B. Tang, R. B. Ji, X. M. Li, G. X. Bai, C. P. Liu, J. H. Hao, J. Y. Lin, H. X. Jiang, K. S. Teng, Z. B. Yang and S. P. Lau, *Acs Nano*, 2014, **8**, 6321.
75 S. J. Zhu, J. H. Zhang, C. Y. Qiao, S. J. Tang, Y. F. Li, W. J. Yuan, B. Li, L. Tian, F. Liu, R. Hu, H. N. Gao, H. T. Wei, H. Zhang, H. C. Sun and B.i Yang, *Chem. Commun.*, 2011, **47**, 6858.
76 X. M. Wen, P. Yu, Y. R. Toh, X. Q. Ma and J. Tang, *Chem. Commun.*, 2014, **50**, 4703.
77 J. Wang, H. Y. Han, X. C. Jiang, L. Huang, L. N. Chen and N. Li, *Anal. Chem.*, 2012, **84**, 4893.
78 Y. Urano, D. Asanum, Y. Ham, Y. Koyam, T. Barrett, M. Kamiy, T. Nagano, T. Watanabe, A. Hasegaw, P. L. Choyke and H. Kobayashi, *Nat. Med.*, 2009, **15**, 1.
79 S. L. Zhu, J. T. Zhang, G. K. Vegesna, R. Pandey, F. T. Luo, S. A. Green and H. Y. Liu, *Chem. Commun.*, 2011, **47**, 3508.
80 S. W Yang and F. Liao, *NANO*, 2011, **6**, 597.
81 A. Coskun, E. H. Deniz and E. U. Akkaya, *Org. Lett.*, 2005, **7**, 5187.
82 Z. S. Qian, X. Y. Shan, L. J. Chai, J. J. Ma, J. R. Chen and H. Feng, *Nanoscale*, 2014, **6**, 5671.
83 P. H. Luo, Z. Ji, C. Li and G. Q. Shi, *Nanoscale*, 2013, **5**, 7361.
84 J. J. Liu, X. L. Zhang, Z. X. Cong, Z. T. Chen, H. H. Yang and G. N. Chen, *Nanoscale*, 2013, **5**, 1810.
85 Q. Lu, W. Wei, Z. X. Zhou, Z. X. Zhou, Y. J. Zhang and S. Q. Liu, *Analyst*, 2014, **139**, 2404.
86 S. Chen, X. Hai, X. W. Chen and J. H. Wang, *Anal. Chem.*, 2014, **86**, 6689.
87 W. H. Nam, B. B. Kim, S. G. Seo, Y. S. Lim, J. Y. Kim, W. S. Seo, W. K. Choi, H. H. Park and J. Y. Lee, *Nano Lett.*, 2014, **14**, 5104.
88 Q. Liu, B. D. Guo, Z. Y. Rao, B. H. Zhang and J. R. Gong, *Nano Lett.*, 2013, **13**, 2436.